HHS Public Access

Author manuscript

J Immunol. Author manuscript; available in PMC 2017 January 01.

Published in final edited form as:

J Immunol. 2016 January 1; 196(1): 407–415. doi:10.4049/jimmunol.1501662.

The mitochondrial phosphatase PGAM5 is dispensable for necroptosis but promotes inflammasome activation in macrophages

Kenta Moriwaki[a,1], **Nivea Farias Luz**[a,d,1], **Sakthi Balaji**[a], **Maria Jose De Rosa**[a,2], **Carey L. O'Donnell**[a], **Peter J. Gough**[c], **John Bertin**[c], **Raymond M. Welsh**[a], and **Francis Ka-Ming Chan**[a]

[a]Department of Pathology, University of Massachusetts Medical School, Worcester, MA 01605, USA

[b]Division of Infectious Diseases and Immunology, University of Massachusetts Medical School, Worcester, MA 01605, USA

[c]Pattern Recognition Receptor Discovery Performance Unit, Immuno-Inflammation Therapeutic Area, GlaxoSmithKline, Collegeville, PA 19422, USA

[d]Centro de Pesquisas Gonçalo Moniz, Fundação Oswaldo Cruz, Universidade Federal da Bahia, Salvador-BA40110-060, Brazil

Abstract

The cytokine IL-1β is intimately linked to many pathological inflammatory conditions. Mature IL-1β secretion requires cleavage by the inflammasome. Recent evidence indicates that many cell death signal adaptors have regulatory roles in inflammasome activity. These include the apoptosis inducers FADD and caspase 8, and the necroptosis kinases receptor interacting protein kinase 1 (RIPK1) and RIPK3. Phosphoglycerate mutase family member 5 (PGAM5) is a mitochondrial phosphatase that has been reported to function downstream of RIPK3 to promote necroptosis and IL-1β secretion. To interrogate the biological function of PGAM5, we generated *Pgam5*$^{-/-}$ mice. We found that *Pgam5*$^{-/-}$ mice were smaller in size compared with wild type littermates, and male *Pgam5*$^{-/-}$ mice were born at sub-Mendelian ratio. Despite these growth and survival defects, *Pgam5*$^{-/-}$ cells responded normally to multiple inducers of apoptosis and necroptosis. Rather, we found that PGAM5 is critical for IL-1β secretion in response to NLRP3 and AIM2 inflammasome agonists. Moreover, vesicular stomatosis virus (VSV)-induced IL-1β secretion was impaired in *Pgam5*$^{-/-}$ bone marrow derived macrophages (BMDMs), but not in *Ripk3*$^{-/-}$ BMDMs, indicating that PGAM5 functions independent of RIPK3 to promote inflammasome activation. Mechanistically, PGAM5 promotes ASC polymerization, maintenance of mitochondrial integrity,

Correspondence: Francis Ka-Ming Chan, Department of Pathology, University of Massachusetts Medical School, AS9-1043, 368 Plantation Street, Worcester, MA 01605, USA.

[1]Equal contribution

[2]Present address: Instituto de Investigaciones Bioquímicas de Bahía Blanca (INIBIBB), CCT-Bahía Blanca-CONICET, Argentina.

The authors have no financial conflicts of interest.

KM and SB generated *Pgam5*$^{-/-}$ mice. KM and MJDR characterized cell death in MEFs and BMDMs, respectively. NFL characterized IL-1β and ROS production, and mitochondrial integrity. SB performed lacZ staining. CLO and RMW assisted with VSV infection. PJG and JB provided critical reagents. FKMC conceived and supervised the project, and wrote the paper.

and optimal ROS production in response to inflammasome signals. Hence, PGAM5 is a novel regulator of inflammasome and caspase 1 activity that functions independently of RIPK3.

Introduction

The inflammatory cytokine IL-1β plays critical roles in protective and pathological inflammation. Mature IL-1β secretion requires two signals. The first signal involves NF-κB-dependent *de novo* synthesis of pro-IL-1β. The second signal typically involves activation of a macromolecular signaling complex called the inflammasome, which consists of sensor proteins such as NLRP3 or AIM2, the adaptor protein ASC, and the IL-1β converting enzyme/protease caspase 1 (1). Activation of the inflammasome and caspase 1 involves prion-like polymerization of the inflammasome (2, 3). Besides caspase 1, pro-IL-1β processing can also be mediated by an alternative caspase 8 activating complex that contains RIPK1, RIPK3 and FADD under certain conditions (4).

Recent discoveries have revealed key sentinel functions of the mitochondria in cell death and inflammation (5). Mitochondria-produced reactive oxygen species (ROS) and release of mitochondrial DNA have been implicated in inflammasome activation (6–8). Phosphoglycerate mutase family member 5 (PGAM5) was originally identified as a substrate of the E3 ligase cullin 2 through its binding to the adaptor Keap1 (9). PGAM5 promotes mitophagy (10, 11), a cellular process that eliminates damaged mitochondria. Furthermore, PGAM5 has been implicated in mitochondria fission through dephosphorylation and activation of the mitochondrial fission protein dynamin related protein 1 (DRP1) (12). The RIPK3-PGAM5-DRP1 axis has been implicated to mediate death receptor- and oxidative stress-induced necrosis (12). In caspase 8-deficient bone marrow derived dendritic cells (BMDCs), PGAM5 was reported to be involved in LPS-induced inflammasome activation and IL-1β secretion (13). However, subsequent shRNA knock-down studies have challenged the role of PGAM5 in necroptosis and IL-1β secretion (14–16).

To definitively evaluate the biology of PGAM5, we generated *Pgam5*-deficient mice. We found that male *Pgam5*$^{-/-}$ mice were born at sub-Mendelian ratio. Moreover, surviving *Pgam5*$^{-/-}$ mice were significantly smaller than their wild type littermates and continued to exhibit reduced viability into adulthood. Despite these growth and survival defects, *Pgam5*$^{-/-}$ cells responded normally to multiple inducers of apoptosis and necroptosis. Rather, we found that *Pgam5*$^{-/-}$ BM-derived macrophages (BMDMs) were highly impaired in inflammasome activation and mature IL-1β secretion. PGAM5 stimulates inflammasome independent of RIPK3, since *Ripk3*$^{-/-}$ and *Ripk3* kinase inactive BMDMs did not exhibit the same defect in IL-1β secretion. In response to inflammasome activation, *Pgam5*$^{-/-}$ BMDMs underwent extensive reduction in mitochondrial volume and produced reduced level of ROS. In wild type BMDMs, PGAM5 translocated to the same detergent-insoluble compartment in which the inflammasome adaptor ASC resides upon stimulation with LPS and the NLRP3 inflammasome agonist nigericin. Moreover, LPS and nigericin induced PGAM5 oligomerization within this detergent-insoluble compartment. Strikingly, oligomerization of the inflammasome adaptors was severely impaired in *Pgam5*$^{-/-}$

BMDMs. These results established PGAM5 as a novel regulator of inflammasome activity that functions independently of RIPK3.

Materials and Methods

Generation of Pgam5-deficient mice

Targeted ES cell clone JM8.N4 (EPD0226_5_H02) was obtained from EUCOMM. Proper recombination was confirmed by Southern blot (Fig. S1A–B). The ES cells were injected to C57BL/6J-Tyr[c-2J]/J (albino-B6) to generate chimeric mice in transgenic animal core at UMMS. Germline transmission of the lacZ allele was confirmed by Southern blot. To generate *Pgam5*$^{fl/+}$ mice, *Pgam5*$^{lacz/+}$ mice were crossed with the flippase transgenic mice (Gt(ROSA)26Sor$^{tm1(Flp1)Dym}$). To generate *Pgam5*$^{-/-}$ mice, *Pgam5*$^{fl/+}$ mice were crossed with mice expressing Cre under the *Sox2* gene promoter. The excision of lacZ/Neo cassette and exon 2 was confirmed by Southern blot. Timed pregnancy test was set up with *Pgam5*$^{-/-}$*Fadd*$^{+/-}$ intercrosses to determine rescue of embryonic lethality of *Fadd*$^{-/-}$ mice. The embryos were fixed in 0.2% glutaraldehyde, 2% formalin, 5 mM EGTA and 2 mM $MgCl_2$ in 0.1 M phosphate buffer (pH 7.3). After rinsing with 0.1% sodium deoxycholate, 0.2% IGEPAL CA-630 (Sigma), 2 mM $MgCl_2$ in 0.1 M phosphate buffer (pH 7.3) for three times, 20 minutes each, the embryos were stained with 1 mg/ml X-gal in potassium ferricyanide and potassium ferrocyanide (5 mM each) dissolved in the rinse solution for overnight at 37°C. The embryos were washed two times with 1X PBS, 15 minutes each the next day. All animal experiments were approved by the institutional animal care and use committee.

Cell Culture

To generate BMDMs, BM cells were cultured in DMEM medium containing 10% fetal bovine serum (FBS), antibiotics, and 20% L929-conditioned medium for 7 days. BMDCs were generated by culture of BM cells in RPMI medium supplemented with 10 ng/ml GM-CSF and 5 ng/ml IL-4 for 7 days. *Asc*$^{-/-}$, *Casp1*$^{-/-}$, *Tnfr1*$^{-/-}$, *Tlr4*$^{-/-}$, *Myd88*$^{-/-}$, *Trif*$^{-/-}$, and *Ripk1*$^{-/-}$ J2 virus-transformed macrophages were cultured in DMEM media containing 10% FBS and antibiotics. Wild type and *Pgam5*$^{-/-}$ MEFs were cultured in DMEM medium containing 10% FBS and antibiotics. *Pgam5*$^{-/-}$ MEFs were transduced with retrovirus carrying SV40 large T antigen/pMSCV and subsequently selected for hygromycin B resistance. SV40-immortalized *Pgam5*$^{-/-}$ MEFs were lentivirally transduced with wild type *Pgam5* isoform 1, isoform 2, and the phosphatase dead mutant (H104A)/pTRIPZ. Transduced cells were selected for puromycin resistance. HepG2 liver cancer cells were transduced with lentivirus expressing shRNA against the *Pgam5* gene (Open Biosystems: #1, V3LHS_312914; #2, V2LHS_62587) and subsequently selected for puromycin resistance. Non-silencing shRNA (Open Biosystems, RHS4346) was used as a control. No sex difference was observed with BMDMs and BMDCs generated from male or female mice.

Measurements of IL-1β secretion

BMDMs were plated a day before stimulation. After 3 hours stimulation with 200 ng/ml ultrapure LPS (InvivoGen), BMDMs were treated with silica (40 μg/ml), nigericin (10 μM)

or ATP (5 mM) for another 3 hours. Poly dA:dT (1 μg/ml) is transfected into cells using lipofectamine 2000 as per manufacturer's instructions. N-acetyl cysteine and Carbonyl cyanide 3-chlorophenylhydrazone (CCCP) were obtained from Calbiochem and Sigma respectively. For VSV infection, BMDMs were primed with 100 ng/ml LPS for 4 hours. After incubation with VSV (Indiana strain, propagated in BHK21 cells, MOI=5) for 2 hours, cells were further incubated for 4 hours before supernatants were harvested. For *in vivo* IL-1β secretion, 5-week old mice were injected with LPS (20 μg/kg) and 700 μg of Alum Imject Adjuvant (Thermo Scientific) in 200 μL PBS i.p. Peritoneal exudates were obtained with 700μL PBS containing 1% FBS two hours after injection. IL-1β secretion in the culture supernatants or the exudates was assessed by ELISA (BD Biosciences).

Quantitative PCR

Total RNA from various organs of 7 week-old mice or BMDMs was used for reverse transcription followed by real-time PCR as described previously (17). *Pgam5* gene expression level in tissues was normalized to the average expression of the two housekeeping genes *Tbp* and *Hprt*. Cytokine expression was normalized to that of *Tbp*. Following primers were used: 5′-TGCCAATGTCATCCGCTAT-3′ and 5′-GGTGATACTGCCGTTGTTGA-3′ for *Pgam5*; 5′-CAAACCCAGAATTGTTCTCCTT-3′ and 5′-ATGTGGTCTTCCTGAATCCCT-3′ for *Tbp*; 5′-TGAAGAGCTACTGTAATGATCAGTCAAC-3′ and 5′-AGCAAGCTTGCAACCTTAACCA-3′ for *Hprt*; 5′-CCCAACTGGTACATCAGCAC-3′ and 5′-TCTGCTCATTCACGAAAAGG -3′ for *Il1b*; 5′-CCCACTCTGACCCCTTTACT -3′ and 5′-TTTGAGTCCTTGATGGTGGT-3′ for *Tnf*; 5′-CGGAGAGGAGACTTCACAGA-3′ and 5′-CCAGTTTGGTAGCATCCATC-3′ for *Il6* and 5′-AGGTGTCCCAAAGAAGCTGTA-3′ and 5′-ATGTCTGGACCCATTCCTTCT-3′ for *Mcp1*.

Western blotting

Whole cell extracts were prepared from various organs of 6 week-old mice or cells using RIPA buffer supplemented with protease inhibitor cocktail (Roche). For BMDMs, whole cell lysates were prepared with standard 1% NP-40 lysis buffer. For chemical crosslinking, cells were treated with 100 ng/mL LPS for 3 hours, followed by 25 μM zVAD-fmk for 30 minutes prior to stimulation with 10 μM nigericin for 30 minutes. Cells were lysed in 1% NP-40, 150 mM NaCl, 20 mM Hepes (pH 7.5) supplemented with protease and phosphatase inhibitor cocktails (Sigma). After centrifugation at 1,800 rpm, supernatant was removed and the insoluble pellet fraction was centrifuged at 5,000 rpm and washed with CHAPS buffer (20 mM Hepes (pH 7.5), 5 mM MgCl2, 0.5 mM EDTA, 0.1 % CHAPS) before chemical crosslinking with 4 mM discuccinimidyl suberate (DSS) (Life Technologies). Reaction was stopped after 30 minutes with Tris-Cl (pH 7.4). Western blotting was performed with antibodies against ASC (N-15, Santa Cruz), caspase 1 (M-20, Santa Cruz), Caspase 8 (1G12, Enzo Life Sciences), PGAM5 (ab126534, Abcam), IL-1β (AF-401-NA, R&D systems), Tom20 (13929, Cell Signaling Technology), Drp1 (8570, Cell Signaling Technology), phopsho-Drp1 Ser637 (4867, Cell Signaling Technology), β-actin (3779, Prosci) and HSP90 (68/Hsp90, BD biosciences) antibodies.

Cell death assay

Cells were pretreated with 10 μM z-VAD-fmk, 0.2 μM BV6, and/or 10 μM Nec-1 for 1 hour before stimulation with TNF or LPS. Hydrogen peroxide (Sigma), rottlerin (Enzo Life Sciences), thapsigargin (Sigma), staurosporine (Enzo Life Sciences), and ABT737 (ApexBio) were used for cell death induction. PGAM5 expression was induced for 24 hours by 1 μg/ml doxycycline (Sigma) before stimulation. Cell death was determined by FACS using propidium iodide and FITC-Annexin V (BD biosciences), CytoTox96 Non-Radioactive Cytotoxicity Assay, CellTiter 96 Aqueous One Solution Cell Proliferation Assay, or CellTiter-Glo Luminescent Cell Viability Assay (Promega).

Measurement of reactive oxygen species (ROS) and mitochondria

Intracellular ROS was detected with the specific fluorescent probe CM-H_2DCFDA (Molecular Probes). BMDMs were primed with 200 ng/ml LPS for 2.5 hours, then loaded with 10 μM CM-H_2DCFDA at 37°C for 30 minutes, exposed to 10 μM nigericin and further incubated for 30 minutes. After washing twice with PBS, the cells were analyzed using LSRII (BD Biosciences). For mitochondria morphology, BMDMs were stained for 30 min with 250 nM Mitotracker Red (Invitrogen) and DAPI (Enzo Life Science). Images were captured using a Leica Microsystems confocal microscope with a 63X objective. For the quantification of mitochondrial surface and volume, the 3D Object counter plugin for the Fiji software (version 2.0) was used (18). Briefly, we used the distance in pixels, the physical distance of the image, and a pixel aspect ratio of 1 to define the pixel size in μm. After defining the threshold between signal and background, the volume and surface of the mitotracker channel is calculated through the image slices.

Statistical analysis

All assays were performed in triplicates and the results represent mean ± SEM. *P* values were calculated with unpaired t test with Welch's correction. *P* values lower than 0.05 are considered statistically significant.

Results

Impaired growth and survival of Pgam5$^{-/-}$ mice

We generated *Pgam5* mutant mice in which the β-galactosidase gene was inserted into the *Pgam5* locus (*Pgam5*$^{lacZ/lacZ}$, Fig. S1A–B). β-gal staining of *Pgam5*$^{lacZ/lacZ}$ embryos revealed that *Pgam5* was highly expressed in the whole epiblast at E7.5 (Fig. S1C). In adult mice, PGAM5 expression could be detected in multiple tissues by Q-PCR and by Western blot (Fig. 1A and 1B). However, residual expression of *Pgam5*, especially in the brain, was still detected in *Pgam5*$^{lacZ/lacZ}$ mice (Fig. 1A). To fully inactivate *Pgam5*, we first crossed *Pgam5*$^{lacZ/lacZ}$ mice to flippase transgenic mice to remove the lacZ cassette, followed by breeding with Sox2-Cre deletor transgenic mice to delete exon 2 of *Pgam5* (Fig. S1A–B). Western blot confirmed that *Pgam5*$^{-/-}$ MEFs and *Pgam5*$^{-/-}$ mice lack PGAM5 expression (Fig. 1B and S1D). Unexpectedly, we found that male *Pgam5*$^{-/-}$ mice, but not female *Pgam5*$^{-/-}$ mice, were born at sub-Mendelian ratio (Fig. 1C). *Pgam5*$^{-/-}$ mice were smaller in size and exhibited reduced body weight compared with their wild type littermates at

weaning age (Fig. 1D and S1E). Consistent with an early growth and survival defect, *Pgam5*$^{-/-}$ mice had a higher mortality rate within the first 100 days (Fig. 1E). These results suggest that PGAM5 is required for optimal growth and organismal survival.

PGAM5 is dispensable for cell death by multiple inducers

PGAM5 was identified as a downstream RIPK3 substrate in necroptosis (12), although more recent studies showed that shRNA knock-down of *Pgam5* did not significantly affect TNF-induced necroptosis (14, 15). To evaluate whether the growth phenotype of *Pgam5*$^{-/-}$ mice is caused by changes in cell death, we tested the response of *Pgam5*$^{-/-}$ cells to various cell death inducers. We found that wild type and *Pgam5*$^{-/-}$ primary MEFs treated with TNF, z-VAD-fmk and the Smac mimetic BV6 exhibited similar level of necroptosis (Fig. 2A). However, since different batches of primary MEFs exhibited a wide range of sensitivity to necroptotic and apoptotic inducers (Fig. S2A–C), we generated SV40-immortalized *Pgam5*$^{-/-}$ MEFs and reconstituted the cells with lentivirus expressing PGAM5 in a doxycycline-inducible manner. Induction of the two wild type mouse PGAM5 isoforms, which differ in a single amino acid residue (Fig. 2B), as well as the phosphatase inactive PGAM5 mutant H104A (19), did not affect TNF, z-VAD-fmk and BV6-induced necroptosis compared with mock-transduced MEFs (Fig. 2C). In addition, TNF and BV6-induced apoptosis was also not affected by expression of PGAM5 (Fig. 2D). Moreover, apoptosis induced by the kinase inhibitor staurosporine (STS) or the Bcl-2 inhibitor ABT737 was also independent of PGAM5 expression (Fig. S2D).

PGAM5 was reported to mediate oxidative stress-induced cell death (12). Contrary to this report, we found that expression of wild type or H104A PGAM5 in *Pgam5*$^{-/-}$ MEFs did not alter cell death induced by hydrogen peroxide, the mitochondrial uncoupler rottlerin, and the ER stress inducer thapsigargin (Fig. S2E). In addition, we found that shRNA-mediated knock-down of PGAM5 did not protect HepG2 cells from acetaminophen-induced cell death (Fig. S2F), a process reported to be mediated by ROS and RIPK3 (20).

In macrophages, LPS and z-VAD-fmk induced necroptosis independent of the inflammasome or autocrine TNF production, but nonetheless required the TLR4 adaptors TRIF and MyD88 and RIPK1 kinase activity (Fig. S3A–C). Consistent with their roles in necroptosis, *Ripk1*$^{-/-}$ and *Ripk3*$^{-/-}$ BMDMs were refractory to LPS and z-VAD-fmk-dependent necroptosis (Fig. 2E) (21). By contrast, *Pgam5*$^{-/-}$ and wild type BMDMs responded similarly to LPS and z-VAD-fmk-induced necroptosis (Fig. 2E). Collectively, the results in figure 2 indicate that PGAM5 is dispensable for cell death triggered by classical apoptosis and necroptosis inducers.

Necroptosis can be induced through mechanisms beyond TNFR1 and TLR4. For example, FADD or caspase 8 deficiency compromised survival of developing embryos through RIPK1 and RIPK3-dependent necroptosis (22–24). However, this event was delayed but not abrogated by inhibiting TNFR-1 or TRIF signaling (25, 26), indicating that developmental necroptosis involves death receptor- and TLR3/4-independent mechanisms. To test the potential role of PGAM5 in developmental necroptosis, we set up timed pregnancy test with *Pgam5*$^{-/-}$*Fadd*$^{+/-}$ mice. At weaning age, no *Pgam5*$^{-/-}$*Fadd*$^{-/-}$ mice was recovered from *Pgam5*$^{-/-}$*Fadd*$^{+/-}$ intercrosses (Table 1). Moreover, the few *Pgam5*$^{-/-}$*Fadd*$^{-/-}$ embryos

that were detected between e10.5–13.5 were highly deformed (data not shown). Hence, we conclude that PGAM5 is dispensable for developmental necroptosis.

PGAM5 promotes optimal IL-1β secretion

In caspase 8-deficient BMDCs, LPS stimulation led to exaggerated IL-1β processing and mature IL-1β secretion in a RIPK3-dependent manner. Knockdown of *Pgam5* expression by shRNA ameliorated the heightened IL-1β secretion by caspase 8-deficient BMDCs (13), suggesting that PGAM5 participates in pro-IL-1β maturation. In contrast, a recent report showed that while RIPK3 is required for pro-IL-1β processing in response to infection by negative strand RNA viruses, shRNA knock-down of PGAM5 did not inhibit RNA virus-induced pro-IL-1β processing (16). To investigate the role of PGAM5 in pro-IL-1β processing, we primed $Pgam5^{fl/fl}$ or $Pgam5^{-/-}$ BMDMs with LPS, followed by stimulation with the NLRP3 inflammasome agonists silica, nigericin, ATP, or the AIM2 inflammasome agonist poly(dA:dT). Surprisingly, $Pgam5^{-/-}$ BMDMs produced reduced level of IL-1β in response to all inflammasome agonists (Fig. 3A and S3D). Time course analysis showed that nigericin-induced IL-1β secretion by $Pgam5^{-/-}$ BMDMs was reduced at all time points tested (Fig. 3B), indicating that the deficiency was not due to delayed response of $Pgam5^{-/-}$ BMDMs. In contrast to BMDMs, $Pgam5^{-/-}$ BMDCs are largely normal for IL-1β secretion (Fig. 3C). The differential requirement of PGAM5 for IL-1β secretion in BMDMs was not caused by differences in cell death, since LPS or LPS and nigericin induced similar level of cell death in $Pgam5^{-/-}$ BMDMs and BMDCs compared with their $Pgam5^{fl/fl}$ counterparts (Fig. 3D). Although mature IL-1β secretion was reduced in $Pgam5^{-/-}$ BMDMs, *Il1b* mRNA expression, as well as that of *Tnf*, *Mcp1* and *Il6*, was normal in $Pgam5^{-/-}$ BMDMs (Fig. 3E). These results suggest that PGAM5 does not regulate cytokine gene transcription, but rather participates in pro-IL-1β processing. Indeed, reduced level of cleaved active caspase 1 was detected in nigericin-treated $Pgam5^{-/-}$ BMDMs (Fig. 3F). In contrast, caspase 8, which has been shown to participate in pro-IL-1β processing in certain conditions (17, 27, 28), was not activated in $Pgam5^{fl/fl}$ and $Pgam5^{-/-}$ BMDMs (Fig. 3F). These results indicate that PGAM5 promotes pro-IL-1β processing through caspase 1-associated inflammasome rather than the recently described RIPK1-RIPK3-FADD-Caspase 8 complex (4).

Inflammasome activation is achieved through polymerization of the complex (2, 3). This process can be measured by isolating the detergent-insoluble fractions from cells and chemical crosslinking to capture higher order ASC oligomers (29). In wild type BMDMs, nigericin-driven ASC oligomerization was detected concomitant with appearance of cleaved caspase 1 (Fig. 3G). In contrast, translocation of ASC to the insoluble compartment and ASC oligomerization was severely blunted in $Pgam5^{-/-}$ BMDMs (Fig. 3G). Moreover, LPS induced translocation of PGAM5 to the detergent-insoluble compartment and PGAM5 oligomerization, which was further enhanced by nigericin treatment (Fig. 3G, compare $(PGAM5)_2$ with $(PGAM5)_1$). Hence, in response to LPS and nigericin, PGAM5 translocates to a detergent-insoluble compartment and undergoes oligomerization to facilitate inflammasome activation.

PGAM5 sustains mitochondrial integrity and ROS production

PGAM5 is a mitochondrial phosphatase that has been implicated to regulate mitochondrial homeostasis (10, 11, 30–32). Consistent with the notion that it is a positive regulator of mitochondrial fission, the mitochondria in *Pgam5*$^{-/-}$ BMDMs appeared to be elongated (Fig. 4A, top panels and white arrow in the inset). This is confirmed when mitochondrial surface and volume were quantified by confocal microscopy (Fig. 4B). However, expression of mitochondrial proteins such as Tom20 and Drp1 was not changed in *Pgam5*$^{-/-}$ BMDMs (Fig. S1D). LPS treatment led to fragmentation of the mitochondria and a concomitant reduction in mitochondrial surface and volume in *Pgam5*$^{-/-}$, but not *Pgam5*$^{fl/fl}$ BMDMs (Fig. 4A, middle panels and insets and Fig. 4B). Nigericin treatment of LPS-stimulated *Pgam5*$^{fl/fl}$ BMDMs led to fragmentation of the mitochondria. In contrast, nigericin did not further increase mitochondrial fragmentation in *Pgam5*$^{-/-}$ BMDMs (Fig. 4A, bottom panels and insets). These results suggest that the mitochondria in *Pgam5*$^{-/-}$ BMDMs are more susceptible to signal-induced perturbations.

Mitochondrial ROS has been implicated in inflammasome activation (6). We found that basal ROS production as determined by the fluorescent dye CM-H_2DCFDA was lower in untreated or LPS-treated *Pgam5*$^{-/-}$ BMDMs (Fig. 5A–B). Nigericin transiently increased ROS production in LPS-primed *Pgam5*$^{-/-}$ BMDMs to a level similar to that in *Pgam5*$^{fl/fl}$ BMDMs (Fig. 5A–B). However, by 30 minutes post-stimulation, ROS level in *Pgam5*$^{-/-}$ BMDMs was again lower than that in *Pgam5*$^{fl/fl}$ BMDMs (Fig. 5A–B), although the difference was not statistically significant. These results suggest that *Pgam5*$^{-/-}$ BMDMs are defective in maintaining high levels of ROS production. Consistent with a role for ROS in IL-1β processing, the anti-oxidant N-acetyl cysteine significantly reduced IL-1β secretion by *Pgam5*$^{fl/fl}$ BMDMs, but not *Pgam5*$^{-/-}$ BMDMs (Fig. 5C). Furthermore, complete depolarization of the mitochondria by the uncoupler CCCP abrogated IL-1β secretion in both *Pgam5*$^{fl/fl}$ and *Pgam5*$^{-/-}$ BMDMs (Fig. 5C). PGAM5 has been implicated to mediate mitochondria fission by dephosphorylating DRP1 at S637 (12). However, dephosphorylation of DRP1 at S637 in response to LPS and nigericin was similar in *Pgam5*$^{fl/fl}$ and *Pgam5*$^{-/-}$ BMDMs (Fig. 5D), suggesting that DRP1 is not a main target of PGAM5 in pro-IL-1β processing.

PGAM5 and RIPK3 regulate IL-1β secretion through distinct pathways

A recent study indicates that RIPK3 acts upstream of DRP-1 to promote double strand RNA (dsRNA)-induced IL-1β secretion (16). However, BMDMs generated from LysM-Cre;*Drp1*$^{fl/fl}$ or *Ripk3*$^{-/-}$ mice do not exhibit defects in dsRNA-induced inflammasome activation (28). We therefore sought to clarify the relationship between RIPK3 and PGAM5 in inflammasome activation and IL-1β secretion. We found that VSV-infected *Ripk3*$^{-/-}$ BMDMs produced normal level of IL-1β (Fig. 5E). In addition, BMDMs derived from knock-in mice expressing kinase inactive *Ripk1* (*Ripk1*$^{kd/kd}$) or *Ripk3* (*Ripk3*$^{kd/kd}$) (33, 34) also produced normal levels of IL-1β in response to VSV (Fig. 5E). By contrast, VSV-induced IL-1β secretion was reduced in *Pgam5*$^{-/-}$ BMDMs (Fig. 5E). Hence, PGAM5 controls inflammasome activation and IL-1β release in BMDMs independent of RIPK1 and RIPK3 function.

We next investigated whether PGAM5 in also required for IL-1β release *in vivo*. Alum injection induces peritonitis and IL-1β release in a NLRP3 inflammasome-dependent manner (35). In this model, *Pgam5*$^{-/-}$ mice produced significantly reduced level of IL-1β compared to wild type mice (Fig. 5F), indicating that PGAM5 is also important for *in vivo* IL-1β release.

Discussion

PGAM5 was originally identified as a mitochondrial phosphatase that controls cellular oxidative stress through binding to the Keap1-Nrf2 complex (9, 36). PGAM5 also binds to Bcl-X_L and thus can indirectly promote Bcl-X_L degradation and sensitize cells to apoptosis (37). In addition, cleaved PGAM5 was implicated in apoptosis (31, 38). In contrast to these pro-apoptotic functions, Drosophila PGAM5 was shown to protect against heat shock-induced apoptosis of the mushroom body (39). The role of PGAM5 in necroptosis is similarly confusing. While it was first reported to be a key substrate of RIPK3 in necroptosis (12), subsequent shRNA knock-down studies did not reveal a prominent role for PGAM5 in necroptosis (14, 15). Using *Pgam5*$^{-/-}$ MEFs and BMDMs, we definitively showed that PGAM5 is dispensable for apoptosis or necroptosis induced by multiple stimuli. This observation is surprising in light of the growth and survival defects of *Pgam5*$^{-/-}$ mice. It is noteworthy that several recent reports have indicated a key role for PGAM5 in mitophagy (10, 11, 30). Accumulation of damaged mitochondria in *Pgam5*$^{-/-}$ mice might contribute to the growth and survival defects. Consistent with this notion, dopaminergic neurons were progressively lost in aging *Pgam5*$^{-/-}$ mice (30).

Although PGAM5 is dispensable for cell death by apoptosis and necroptosis, it has a critical role in processing of pro-IL-1β in BMDMs. IL-1β is a key inflammatory cytokine with wide-ranging effects in immune responses and many inflammatory diseases. In this study, we showed that the mitochondrial phosphatase PGAM5 is dispensable for necroptosis and apoptosis, but has a crucial role in optimal IL-1β secretion by BMDMs in response to multiple inflammasome agonists. This effect is achieved through caspase 1-mediated cleavage of pro-IL-1β, as inflammasome assembly was severely impaired in *Pgam5*$^{-/-}$ BMDMs. PGAM5 likely controls inflammasome activation indirectly, since we did not detect direct physical interaction between PGAM5 and ASC (data not shown). However, PGAM5 was found in the same detergent-insoluble compartment as the inflammasome. Unlike ASC, which only translocated to the detergent-insoluble compartment in response to nigericin, LPS alone triggered PGAM5 translocation to this compartment. PGAM5 accumulation and oligomerization in this compartment was further enhanced by nigericin. Mitochondria-produced ROS has been implicated in inflammasome activation (6). Consistent with PGAM5's proposed role in mitochondrial fission, the mitochondria in *Pgam5*$^{-/-}$ BMDMs were elongated with increased volume and surface. *Pgam5*$^{-/-}$ BMDMs underwent mitochondrial fragmentation in response to LPS, suggesting that PGAM5 has important functions in maintaining mitochondrial homeostasis. Consistent with this notion, we found that *Pgam5*$^{-/-}$ BMDMs were impaired in ROS production. However, the effect of PGAM5 deficiency on LPS and nigericin-induced ROS production was modest and not statistically significant. This suggests that other mechanisms might be involved in PGAM5-mediated inflammasome activation.

Emerging evidence indicates that cell death signal adaptors often have dual roles in inflammation (40, 41). In particular, the apoptosis adaptors FADD and caspase 8, and the necroptosis adaptors RIPK1 and RIPK3, can regulate inflammasome activity in both BMDMs and BMDCs (13, 17, 27, 28). The mechanism employed by these cell death adaptors to control pro-IL-1β processing varies greatly depending on the cell type and stimulus used. For example, caspase 8 can complex with FADD, RIPK1 and RIPK3 to directly cleave pro-IL-1β (4, 17). When caspase 8 activity is inhibited, this complex can in turn recruits MLKL to promote IL-1β maturation through a yet to be defined mechanism (27, 28). Interestingly, RIPK3 was reported to stimulate NLRP3 inflammasome activation via PGAM5 in caspase 8-deficient DCs (13). In wild type BMDMs, however, we found that PGAM5, but not RIPK3, was required for optimal inflammasome activation and VSV-induced IL-1β secretion by BMDMs. This is in contrast to a recent report, which showed that RIPK3, but not PGAM5, has an essential role in RNA virus-induced IL-1β secretion in LPS-primed BMDMs (16). The reason for these discrepant observations is unknown at present, but may be related to efficiency of shRNA knockdown of PGAM5 in different studies. Rather, our results are consistent with a more recent report showing that RIPK3 is dispensable for dsRNA or VSV-induced inflammasome activation (28). Nonetheless, the inflammasome-stimulating activity of RIPK3 is unleashed regardless of the cell type used when cellular IAPs, FADD or caspase 8 are inhibited (27). Under these conditions, RIPK3 and PGAM5 may cooperate with each other to stimulate inflammasome activity and pro-IL-1β processing. As PGAM5 facilitates activation of multiple inflammasomes, it will be interesting to determine if targeting PGAM5 is a viable therapeutic strategy in IL-1β driven inflammatory diseases.

Supplementary Material

Refer to Web version on PubMed Central for supplementary material.

Acknowledgments

This work is supported by NIH grant AI083497 (F.K.M. Chan). K.M. was supported by postdoctoral fellowships from the Uehara Memorial Foundation and the Japan Society for the Promotion of Science. N.F.L. receives a fellowship from National Council for Scientific and Technological Development (Brazil).

We thank Stephen Jones for providing the flippase and Cre deletor mice.

Literature cited

1. Lamkanfi M V, Dixit M. Mechanisms and functions of inflammasomes. Cell. 2014; 157:1013–1022. [PubMed: 24855941]
2. Lu A V, Magupalli G, Ruan J, Yin Q, Atianand MK, Vos MR, Schroder GF, Fitzgerald KA, Wu H, Egelman EH. Unified polymerization mechanism for the assembly of ASC-dependent inflammasomes. Cell. 2014; 156:1193–1206. [PubMed: 24630722]
3. Cai X, Chen J, Xu H, Liu S, Jiang QX, Halfmann R, Chen ZJ. Prion-like polymerization underlies signal transduction in antiviral immune defense and inflammasome activation. Cell. 2014; 156:1207–1222. [PubMed: 24630723]
4. Moriwaki K, Bertin J, Gough PJ, Chan FK. A RIPK3-caspase 8 complex mediates atypical pro-IL-1beta processing. J Immunol. 2015; 194:1938–1944. [PubMed: 25567679]
5. Gurung P, Lukens JR, Kanneganti TD. Mitochondria: diversity in the regulation of the NLRP3 inflammasome. Trends in molecular medicine. 2015; 21:193–201. [PubMed: 25500014]

6. Zhou R, Yazdi AS, Menu P, Tschopp J. A role for mitochondria in NLRP3 inflammasome activation. Nature. 2011; 469:221–225. [PubMed: 21124315]
7. Nakahira K, Haspel JA, Rathinam VA, Lee SJ, Dolinay T, Lam HC, Englert JA, Rabinovitch M, Cernadas M, Kim HP, Fitzgerald KA, Ryter SW, Choi AM. Autophagy proteins regulate innate immune responses by inhibiting the release of mitochondrial DNA mediated by the NALP3 inflammasome. Nature immunology. 2011; 12:222–230. [PubMed: 21151103]
8. Shimada K, Crother TR, Karlin J, Dagvadorj J, Chiba N, Chen S, Ramanujan VK, Wolf AJ, Vergnes L, Ojcius DM, Rentsendorj A, Vargas M, Guerrero C, Wang Y, Fitzgerald KA, Underhill DM, Town T, Arditi M. Oxidized mitochondrial DNA activates the NLRP3 inflammasome during apoptosis. Immunity. 2012; 36:401–414. [PubMed: 22342844]
9. Lo SC, Hannink M. PGAM5, a Bcl-XL-interacting protein, is a novel substrate for the redox-regulated Keap1-dependent ubiquitin ligase complex. J Biol Chem. 2006; 281:37893–37903. [PubMed: 17046835]
10. Chen G, Han Z, Feng D, Chen Y, Chen L, Wu H, Huang L, Zhou C, Cai X, Fu C, Duan L, Wang X, Liu L, Liu X, Shen Y, Zhu Y, Chen Q. A regulatory signaling loop comprising the PGAM5 phosphatase and CK2 controls receptor-mediated mitophagy. Molecular cell. 2014; 54:362–377. [PubMed: 24746696]
11. Wu H, Xue D, Chen G, Han Z, Huang L, Zhu C, Wang X, Jin H, Wang J, Zhu Y, Liu L, Chen Q. The BCL2L1 and PGAM5 axis defines hypoxia-induced receptor-mediated mitophagy. Autophagy. 2014; 10:1712–1725. [PubMed: 25126723]
12. Wang Z, Jiang H, Chen S, Du F, Wang X. The mitochondrial phosphatase PGAM5 functions at the convergence point of multiple necrotic death pathways. Cell. 2012; 148:228–243. [PubMed: 22265414]
13. Kang TB, Yang SH, Toth B, Kovalenko A, Wallach D. Caspase-8 blocks kinase RIPK3-mediated activation of the NLRP3 inflammasome. Immunity. 2013; 38:27–40. [PubMed: 23260196]
14. Murphy JM, Czabotar PE, Hildebrand JM, Lucet IS, Zhang JG, Alvarez-Diaz S, Lewis R, Lalaoui N, Metcalf D, Webb AI, Young SN, Varghese LN, Tannahill GM, Hatchell EC, Majewski IJ, Okamoto T, Dobson RC, Hilton DJ, Babon JJ, Nicola NA, Strasser A, Silke J, Alexander WS. The pseudokinase MLKL mediates necroptosis via a molecular switch mechanism. Immunity. 2013; 39:443–453. [PubMed: 24012422]
15. Remijsen Q, Goossens V, Grootjans S, Van den Haute C, Vanlangenakker N, Dondelinger Y, Roelandt R, Bruggeman I, Goncalves A, Bertrand MJ, Baekelandt V, Takahashi N, Berghe TV, Vandenabeele P. Depletion of RIPK3 or MLKL blocks TNF-driven necroptosis and switches towards a delayed RIPK1 kinase-dependent apoptosis. Cell death & disease. 2014; 5:e1004. [PubMed: 24434512]
16. Wang X, Jiang W, Yan Y, Gong T, Han J, Tian Z, Zhou R. RNA viruses promote activation of the NLRP3 inflammasome through a RIP1-RIP3-DRP1 signaling pathway. Nature immunology. 2014; 15:1126–1133. [PubMed: 25326752]
17. Moriwaki K, Balaji S, McQuade T, Malhotra N, Kang J, Chan FK. The Necroptosis Adaptor RIPK3 Promotes Injury-Induced Cytokine Expression and Tissue Repair. Immunity. 2014; 41:567–578. [PubMed: 25367573]
18. Bolte S, Cordelieres FP. A guided tour into subcellular colocalization analysis in light microscopy. Journal of microscopy. 2006; 224:213–232. [PubMed: 17210054]
19. Takeda K, Komuro Y, Hayakawa T, Oguchi H, Ishida Y, Murakami S, Noguchi T, Kinoshita H, Sekine Y, Iemura S, Natsume T, Ichijo H. Mitochondrial phosphoglycerate mutase 5 uses alternate catalytic activity as a protein serine/threonine phosphatase to activate ASK1. Proceedings of the National Academy of Sciences of the United States of America. 2009; 106:12301–12305. [PubMed: 19590015]
20. Ramachandran A, McGill MR, Xie Y, Ni HM, Ding WX, Jaeschke H. Receptor interacting protein kinase. 3 is a critical early mediator of acetaminophen-induced hepatocyte necrosis in mice. Hepatology. 2013; 58:2099–2108. [PubMed: 23744808]
21. He S, Liang Y, Shao F, Wang X. Toll-like receptors activate programmed necrosis in macrophages through a receptor-interacting kinase-3-mediated pathway. Proceedings of the National Academy of Sciences of the United States of America. 2011; 108:20054–20059. [PubMed: 22123964]

22. Kaiser WJ, Upton JW, Long AB, Livingston-Rosanoff D, Daley-Bauer LP, Hakem R, Caspary T, Mocarski ES. RIP3 mediates the embryonic lethality of caspase-8-deficient mice. Nature. 2011; 471:368–372. [PubMed: 21368762]

23. Oberst A, Dillon CP, Weinlich R, McCormick LL, Fitzgerald P, Pop C, Hakem R, Salvesen GS, Green DR. Catalytic activity of the caspase-8-FLIP(L) complex inhibits RIPK3-dependent necrosis. Nature. 2011; 471:363–367. [PubMed: 21368763]

24. Zhang H, Zhou X, McQuade T, Li J, Chan FK, Zhang J. Functional complementation between FADD and RIP1 in embryos and lymphocytes. Nature. 2011; 471:373–376. [PubMed: 21368761]

25. Dillon CP, Oberst A, Weinlich R, Janke LJ, Kang TB, Ben-Moshe T, Mak TW, Wallach D, Green DR. Survival function of the FADD-CASPASE-8-cFLIP(L) complex. Cell reports. 2012; 1:401–407. [PubMed: 22675671]

26. Dillon CP, Weinlich R, Rodriguez DA, Cripps JG, Quarato G, Gurung P, Verbist KC, Brewer TL, Llambi F, Gong YN, Janke LJ, Kelliher MA, Kanneganti TD, Green DR. RIPK1 blocks early postnatal lethality mediated by caspase-8 and RIPK3. Cell. 2014; 157:1189–1202. [PubMed: 24813850]

27. Lawlor KE, Khan N, Mildenhall A, Gerlic M, Croker BA, D'Cruz AA, Hall C, Kaur Spall S, Anderton H, Masters SL, Rashidi M, Wicks IP, Alexander WS, Mitsuuchi Y, Benetatos CA, Condon SM, Wong WW, Silke J, Vaux DL, Vince JE. RIPK3 promotes cell death and NLRP3 inflammasome activation in the absence of MLKL. Nature communications. 2015; 6:6282.

28. Kang S, Fernandes-Alnemri T, Rogers C, Mayes L, Wang Y, Dillon C, Roback L, Kaiser W, Oberst A, Sagara J, Fitzgerald KA, Green DR, Zhang J, Mocarski ES, Alnemri ES. Caspase-8 scaffolding function and MLKL regulate NLRP3 inflammasome activation downstream of TLR3. Nature communications. 2015; 6:7515.

29. Yu JW, Fernandes-Alnemri T, Datta P, Wu J, Juliana C, Solorzano L, McCormick M, Zhang Z, Alnemri ES. Pyrin activates the ASC pyroptosome in response to engagement by autoinflammatory PSTPIP1 mutants. Molecular cell. 2007; 28:214–227. [PubMed: 17964261]

30. Lu W, Karuppagounder SS, Springer DA, Allen MD, Zheng L, Chao B, Zhang Y, Dawson VL, Dawson TM, Lenardo M. Genetic deficiency of the mitochondrial protein PGAM5 causes a Parkinson's-like movement disorder. Nature communications. 2014; 5:4930.

31. Sekine S, Kanamaru Y, Koike M, Nishihara A, Okada M, Kinoshita H, Kamiyama M, Maruyama J, Uchiyama Y, Ishihara N, Takeda K, Ichijo H. Rhomboid protease PARL mediates the mitochondrial membrane potential loss-induced cleavage of PGAM5. J Biol Chem. 2012; 287:34635–34645. [PubMed: 22915595]

32. Imai Y, Kanao T, Sawada T, Kobayashi Y, Moriwaki Y, Ishida Y, Takeda K, Ichijo H, Lu B, Takahashi R. The loss of PGAM5 suppresses the mitochondrial degeneration caused by inactivation of PINK1 in Drosophila. PLoS genetics. 2010; 6:e1001229. [PubMed: 21151955]

33. Berger S, Kasparcova V, Hoffman S, Swift B, Dare L, Schaeffer M, Capriotti C, Cook M, Finger J, Hughes-Earle A, Harris P, Kaiser WJ, Mocarski ES, Bertin J, Gough P. Cutting Edge: RIP1 Kinase Activity is Dispensable for Normal Development but is a Key Regulator of Inflammation in SHARPIN-Deficient Mice. J Immunol. 2014

34. Mandal P, Berger SB, Pillay S, Moriwaki K, Huang C, Guo H, Lich JD, Finger J, Kasparcova V, Votta B, Ouellette M, King BW, Wisnoski D, Lakdawala AS, DeMartino MP, Casillas LN, Haile PA, Sehon CA, Marquis RW, Upton J, Daley-Bauer LP, Roback L, Ramia N, Dovey CM, Carette JE, Chan FK, Bertin J, Gough PJ, Mocarski ES, Kaiser WJ. RIP3 Induces Apoptosis Independent of Pronecrotic Kinase Activity. Molecular cell. 2014; 56:481–495. [PubMed: 25459880]

35. Eisenbarth SC, Colegio OR, O'Connor W, Sutterwala FS, Flavell RA. Crucial role for the Nalp3 inflammasome in the immunostimulatory properties of aluminium adjuvants. Nature. 2008; 453:1122–1126. [PubMed: 18496530]

36. Lo SC, Hannink M. PGAM5 tethers a ternary complex containing Keap1 and Nrf2 to mitochondria. Experimental cell research. 2008; 314:1789–1803. [PubMed: 18387606]

37. Niture SK, Jaiswal AK. Inhibitor of Nrf2 (INrf2 or Keap1) protein degrades Bcl-xL via phosphoglycerate mutase 5 and controls cellular apoptosis. J Biol Chem. 2011; 286:44542–44556. [PubMed: 22072718]

38. Zhuang M, Guan S, Wang H, Burlingame AL, Wells JA. Substrates of IAP ubiquitin ligases identified with a designed orthogonal E3 ligase, the NEDDylator. Molecular cell. 2013; 49:273–282. [PubMed: 23201124]

39. Ishida Y, Sekine Y, Oguchi H, Chihara T, Miura M, Ichijo H, Takeda K. Prevention of apoptosis by mitochondrial phosphatase PGAM5 in the mushroom body is crucial for heat shock resistance in Drosophila melanogaster. PloS one. 2012; 7:e30265. [PubMed: 22347370]

40. Chan FK, Luz NF, Moriwaki K. Programmed necrosis in the cross talk of cell death and inflammation. Annual review of immunology. 2015; 33:79–106.

41. Silke J, Rickard JA, Gerlic M. The diverse role of RIP kinases in necroptosis and inflammation. Nature immunology. 2015; 16:689–697. [PubMed: 26086143]

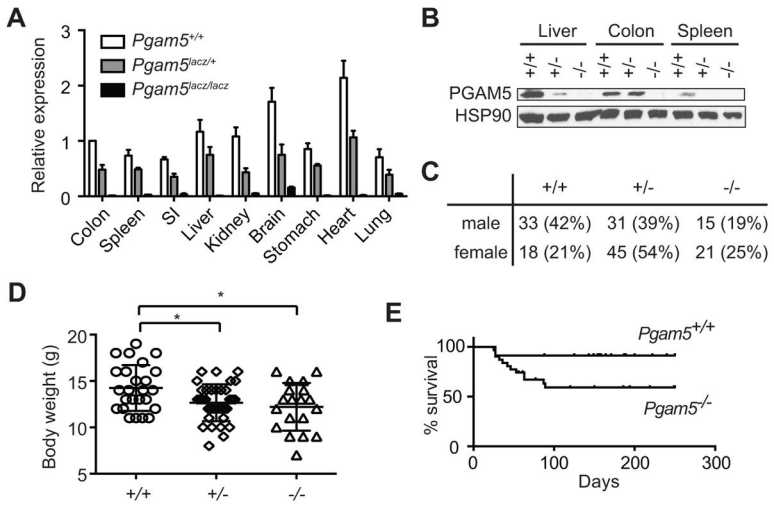

Figure 1. *Pgam5*$^{-/-}$ mice are born at sub-Mendelian ratio and exhibit reduced body weight

(**A**) Pgam5 expression from various tissues of 7 week old mice was determined by real-time PCR. SI, small intestine. (**B**) PGAM5 protein expression in the indicated tissues was determined by Western blot. (**C**) Male *Pgam5*$^{-/-}$ mice were born at sub-Mendelian ratio. The number of progenies from *Pgam5*$^{+/-}$ intercrosses with the indicated genotypes was shown. The percentages are shown in parentheses. (**D**) *Pgam5*$^{-/-}$ mice exhibit reduced body weight. Body weight of mice with the indicated genotypes from *Pgam5*$^{+/-}$ intercross was determined on day 28 after birth. *Pgam5*$^{+/+}$ (n=25), *Pgam5*$^{+/-}$ (n=35), *Pgam5*$^{-/-}$ (n=19). Bars: mean ± SEM. * $p \leq 0.01$. (**E**) *Pgam5*$^{-/-}$ mice exhibit increased mortality. *Pgam5*$^{+/+}$ (n=22), *Pgam5*$^{-/-}$ (n=30).

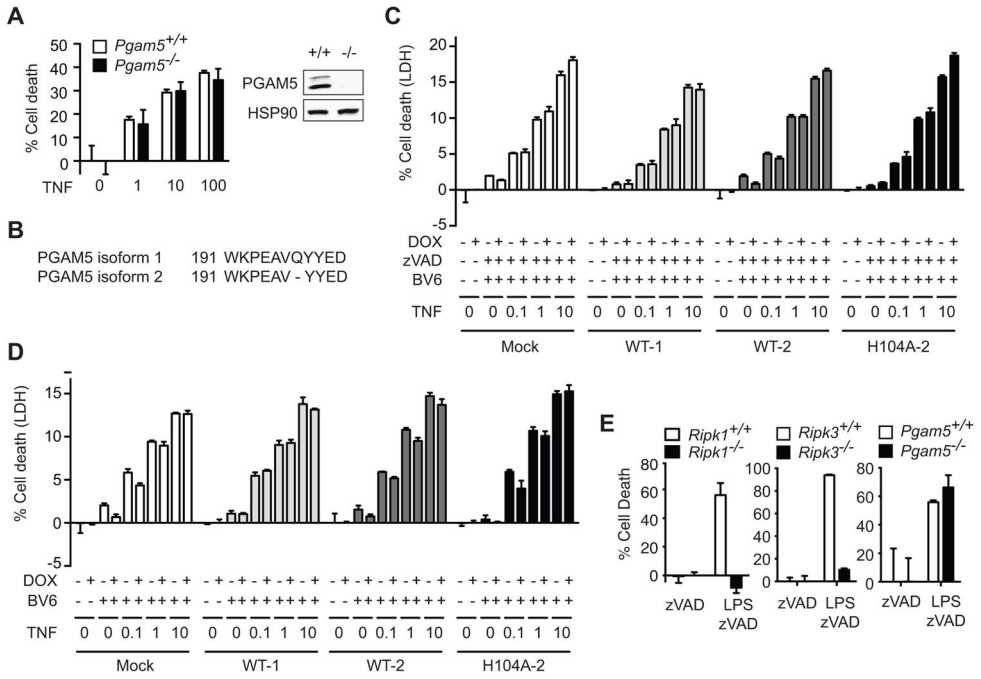

Figure 2. PGAM5 is dispensable for necroptosis and apoptosis

(**A**) Primary MEFs were stimulated with the indicated amount of TNF (ng/ml), 10 μM z-VAD-fmk (zVAD) and 0.2 μM BV6 for 24 hours. Western blot shows that PGAM5 expression was abolished in *Pgam5*$^{-/-}$ MEFs. (**B**) Sequence alignment of mouse PGAM5 isoform 1 and 2 shows that the two isoforms differ in a single glutamine residue that is absent in isoform 2. (**C and D**) SV40-transformed *Pgam5*$^{-/-}$ MEFs transduced with PGAM5 wild type isoform 1 (WT-1), isoform 2 (WT-2), or phosphatase-dead mutant of isoform 2 (H104A-2) were stimulated with indicated amount of TNF (ng/ml) in the presence of 0.2 μM BV6 and/or 10 μM zVAD. (**E**) *Ripk1*$^{-/-}$ and *Ripk3*$^{-/-}$ J2-virus transformed macrophages and *Pgam5*$^{-/-}$ BMDMs were stimulated with 100 ng/ml LPS and 10 μM zVAD for 12 hours. Cell death was determined as described in materials and methods. Results shown are mean ± SEM.

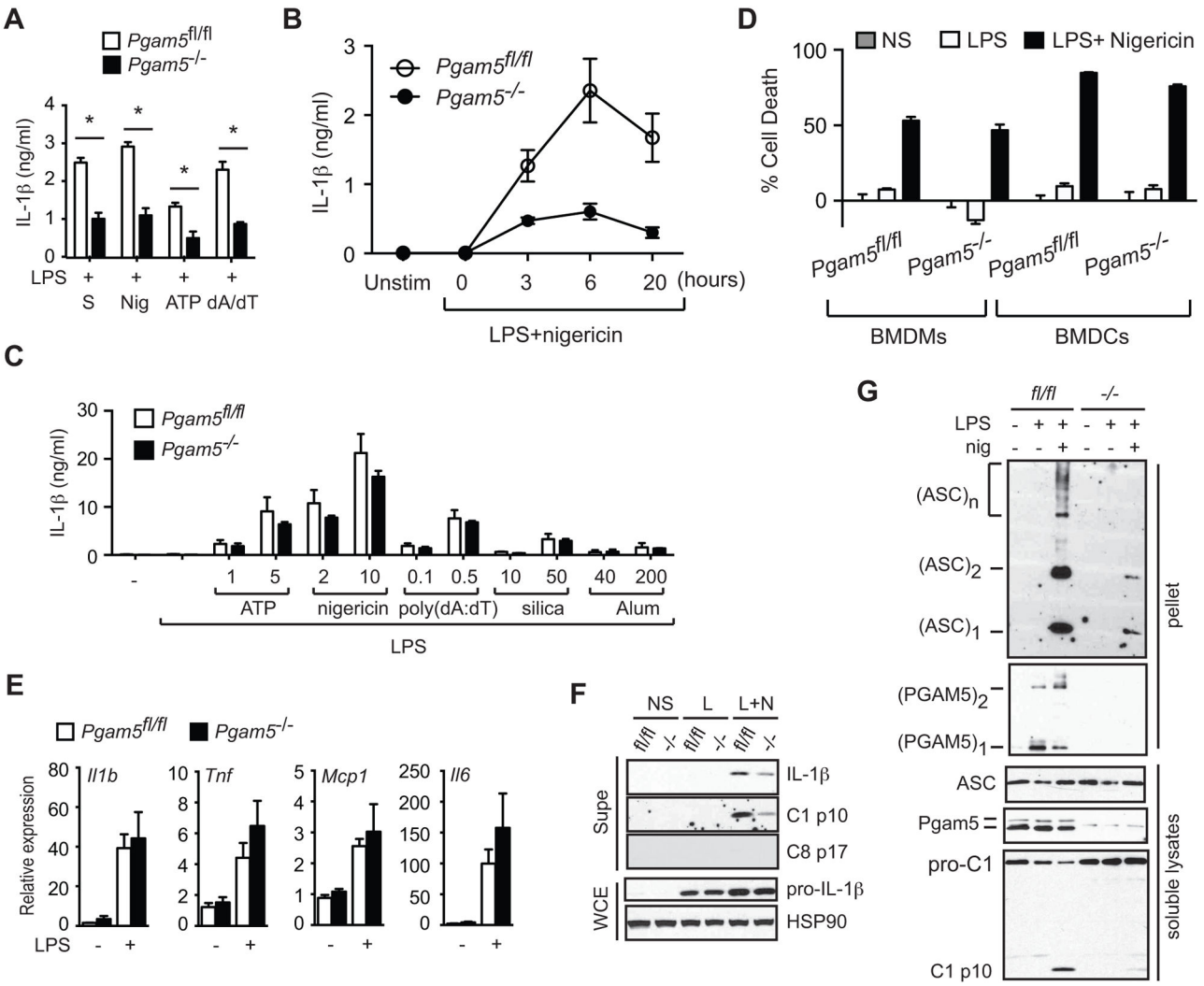

Figure 3. PGAM5 is required for optimal caspase 1 activation and IL-1β secretion

(**A**) LPS-primed BMDMs were stimulated with the silica (S), nigericin (Nig), ATP or poly(dA:dT) (dA/dT) for 3 hours. IL-1 β secretion was determined by ELISA. (**B**) Kinetic measurements of IL-1β secretion by LPS-primed BMDMs treated with nigericin for the indicated amount of time. (**C**) PGAM5 is dispensable for IL-1β secretion in BMDCs. BMDCs were primed with 10 ng/ml LPS for 3 hours and the indicated concentrations of ATP (mM), nigericin (μM), silica (μg/ml), alum (μg/ml) or poly(dA:dT) (μg/ml) for another 3 hours prior to ELISA detection of secreted IL-1β detection in the culture media. (**D**) PGAM5 deficiency did not affect cell death induced by LPS or LPS+nigericin in BMDMs and BMDCs. Cells primed with 200 ng/ml LPS for 3 hours were stimulated with 10 μM nigericin for 3 hours. Cell death was determined by CellTiter-Glo Luminescent Cell Viability Assay. (**E**) BMDMs were stimulated with LPS for 3 hours and cytokine expression was determined by Q-PCR. (**F–G**) *Pgam5*$^{fl/fl}$ or *Pgam5*$^{-/-}$ BMDMs were stimulated with LPS (L) for 3 hours, followed by 10 μM nigericin (N) for 30 minutes. Whole cell extracts (WCE) or supernatants (Supe) were subjected to Western blot (**F**). The detergent insoluble fraction was subjected to chemical crosslinking as described in methods (**G**). Monomers,

dimers and oligomers of ASC and PGAM5 were shown (**G**). Results shown are mean ± SEM. * $p \leq 0.05$.

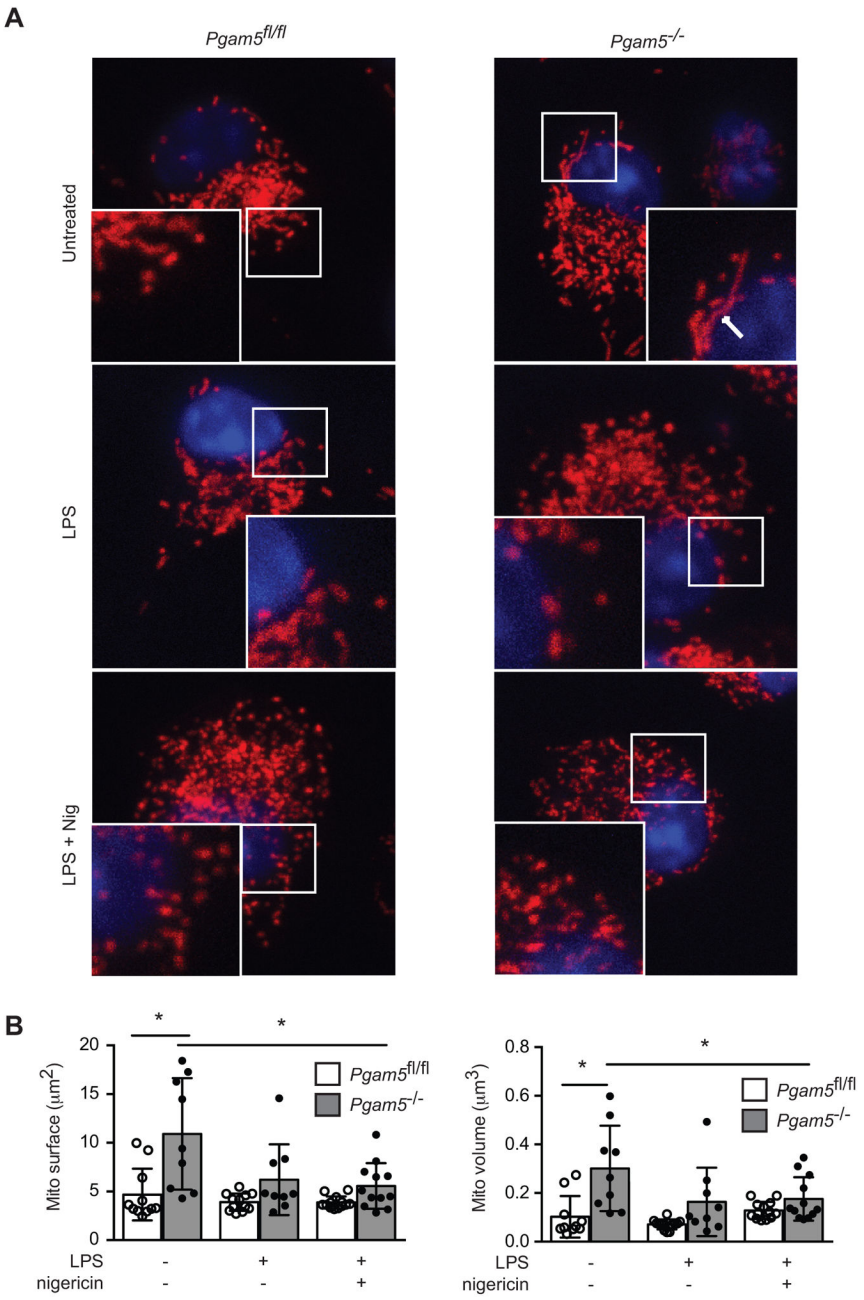

Figure 4. PGAM5 regulates mitochondrial homeostasis

(**A**) Mitotracker red staining of *Pgam5*$^{fl/fl}$ and *Pgam5*$^{-/-}$ BMDMs treated with LPS or LPS and nigericin. Red=mitotracker red, blue=DAPI. A magnified version of the indicated area of interest is shown in the inset. The white arrow in the inset shows an elongated mitochondria. (**B**) Mitochondrial surface and volume were quantified for *Pgam5*$^{fl/fl}$ and *Pgam5*$^{-/-}$ BMDMs using the 3D Object counter plugin for the Fiji software (version 2.0) and Image J as described in materials and method (18). Results shown are mean ± SEM. * $p \leq 0.05$.

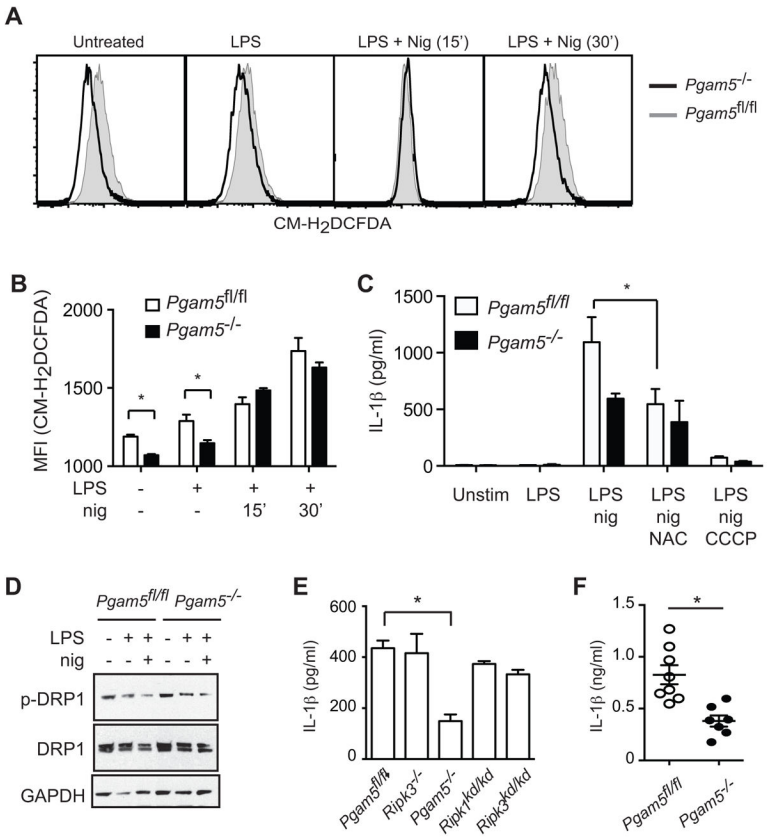

Figure 5. PGAM5, but not RIPK3, is required for VSV-induced IL-1β secretion

(**A**) Untreated, LPS-treated, or LPS and nigericin-treated BMDMs from *Pgam5*$^{fl/fl}$ (shaded curves) and *Pgam5*$^{-/-}$ (bold curves) mice were monitored for ROS production using the fluorescent probe CM-H_2DCFDA. (**B**) Mean fluorescence intensity (MFI) of CM-H2DCFDA staining of BMDMs treated under the indicated conditions. (**C**) BMDMs were treated with LPS and nigericin as described in materials and methods. Where indicated, the cells were pre-treated 20 mM NAC or 50 μM CCCP for 30 minutes prior to addition of nigericin. IL-1β secretion was measured 3 hours after nigericin treatment. (**D**) BMDMs were treated with LPS for 3 hours, followed by nigericin for 30 minutes. DRP1 phosphorylation at S637 was detected by Western blot as indicated. (**E**) LPS-primed BMDMs of the indicated genotypes were infected with VSV for 6 hours. IL-1β release was determined by ELISA. (**F**) *Pgam5* $^{fl/fl}$ (n=8) and *Pgam5*$^{-/-}$ (n=7) mice were injected i.p. with LPS and Alum for 2 hours and IL-β in the peritoneal exudate was determined by ELISA. Results shown are mean ± SEM. * $p \leq 0.05$.

Table 1

Number of progenies of each genotype from *Pgam5*$^{-/-}$*Fadd*$^{+/-}$ intercrosses.

	Pgam5$^{-/-}$**Fadd**$^{+/+}$	**Pgam5**$^{-/-}$**Fadd**$^{+/-}$	**Pgam5**$^{-/-}$**Fadd**$^{-/-}$
E10.5–13.5	11	20	5
D28	12	25	0